Nitric Oxide Reduces the Sequestration of Polymorphonuclear Leukocytes in Lung by Changing Deformability and CD18 Expression

YUKIO SATO, KEITH R. WALLEY, MARIA E. KLUT, DEAN ENGLISH, YULIA D'YACHKOVA, JAMES C. HOGG, and STEPHAN F. van EEDEN

University of British Columbia Pulmonary Research Laboratory, St. Paul's Hospital, Vancouver, British Columbia, Canada

Nitric oxide (NO) influences polymorphonuclear leukocytes (PMN)–endothelial cell interactions. The aim of this study was to evaluate this effect in the lung and investigate this mechanism. PMN sequestration in the lung was evaluated *in vivo* after the infusion of complement fragments. Rabbits ($n = 9$) that inhaled 40 ppm of NO were compared with control rabbits ($n = 9$) over a 2-h period following infusion of complement fragments. Circulating PMN counts immediately decreased after infusion of complement fragments in both groups followed by a recovery to baseline. This recovery was maintained in the NO-treated group compared with the control rabbits ($p < 0.05$). NO reduced PMN sequestration in the lung measured by both arteriovenous PMN difference across the lung ($p < 0.01$) and the myeloperoxidase (MPO) content of the lung tissue ($p < 0.01$). NO had no effect on the complement fragments–induced PMN release from the bone marrow. *In vitro* studies showed that NO partially inhibited F-actin assembly ($p < 0.01$) reduced the change in deformability ($p < 0.05$) and inhibited CD18 upregulation ($p < 0.05$) but had no effect on the L-selectin shedding of PMN stimulated by complement fragments. We conclude that NO reduces the sequestration of activated PMN by reducing deformability change via inhibition of F-actin assembly and inhibiting the upregulation of CD18. Sato Y, Walley KR, Klut ME, English D, D'yachkova Y, Hogg JC, van Eeden SF. Nitric oxide reduces the sequestration of polymorphonuclear leukocytes in lung by changing deformability and CD18 expression. AM J RESPIR CRIT CARE MED 1999;159:1469–1476.

Polymorphonuclear leukocytes (PMN) play an important role in the pathogenesis of the lung injury responsible for the acute respiratory distress syndrome (1–3). The initiating event in the development of the injury is PMN sequestration in microvessels of the lung (3). Factors that have been proposed to be responsible for the PMN sequestration in the lung are the size and deformability of PMN as well as the adhesive qualities of PMN and endothelial cells (4). PMN are concentrated in the lung microvascular bed with respect to red blood cells (RBC), because of discrepancies in the size between PMN and pulmonary capillaries and the deformability of PMN (1). PMN and RBC have similar diameters, but differences in the deformability between PMN and RBC result in mean pulmonary transit times of approximately 190 s for PMN compared with approximately 3 s for RBC (5). The multisegmental nature of the pulmonary capillary bed allows RBC to stream around the slower moving PMN and form a large marginated pool of PMN in the lung (1, 5).

(*Received in original form August 14, 1998 and in revised form November 19, 1998*)

Supported by Grant 4219 of the Medical Research Council of Canada.

Correspondence and requests for reprints should be addressed to Dr. Stephan van Eeden, Pulmonary Research Laboratory, St. Paul's Hospital, Vancouver, BC, V6Z 1Y6 Canada. E-mail: SVANEEDEN@PRL. Pulmonary. UBC. CA

Am J Respir Crit Care Med Vol 159. pp 1469–1476, 1999
Internet address: www.atsjournals.org

Inflammatory stimuli further increase PMN transit time by decreasing their deformability and increasing their adhesiveness to endothelial cells. The decrease in deformability is mediated by a rapid assembly of filamentous F-actin from soluble G-actin at the cell periphery which increases the rigidity and viscosity of PMN, which further increase PMN transit time through the lung (6–8). This increased PMN transit time results in further concentration of PMN in the lung. Adherence between PMN and endothelial cells is influenced by adhesion molecules. The selectins slow PMN by mediating rolling; the integrins induce firm adhesion between PMN and endothelial cells (4). The interaction between these adhesion molecules on PMN and their ligands on endothelial cells contributes to prolonged PMN sequestration in the lung (4, 9). Finally, PMN release from the bone marrow by inflammatory stimuli also affects PMN sequestration in the lung, because the bone marrow has a large pool of PMN and because PMN newly released from the bone marrow preferentially sequester in the lung microvessels (10–13).

Nitric oxide (NO) is a biologically active compound synthesized from L-arginine that regulates various cellular functions. NO causes smooth muscle cell relaxation by stimulating guanylate cyclase in vascular smooth muscle cells to generate cyclic guanosine monophosphate (cGMP) (14, 15). There is growing evidence indicating that NO influences inflammatory response by modulating PMN–endothelial cell interactions (16, 17). Inhibition of NO synthesis using NO synthase inhibitors increases PMN adhesion to mesenteric venules of cats (18), increases the number of PMN in granulomatous inflam-

mation of mouse lung (19), increases PMN sequestration in the lung of rats (20) and in the heart of cats (21), and increases microvascular permeability in small intestine of cats (22). Conversely, administration of exogenous NO prevents PMN adhesion to mesenteric venules of cats (18), decreases PMN sequestration in isolated lung of rats (23, 24), and attenuates lung injury in pigs (25). However, the mechanisms of the inhibitory effect of NO on PMN–endothelial interaction are not clear.

Our working hypothesis is that NO reduces PMN sequestration in the lung by altering PMN function. The aim of this study is to evaluate the effect of NO on PMN both *in vivo* and *in vitro* using a well established model of PMN sequestration in the lung. The effects of inhaled NO on PMN sequestration in the lung and PMN release from the bone marrow were examined after infusion of complement fragment into rabbits. The effects of NO on F-actin assembly, deformability change, and adhesion molecule expression of activated PMN were examined *in vitro* to explore the mechanisms of reduced PMN sequestration by inhaled NO *in vivo*.

METHODS

In Vivo Study

Animals. Female New Zealand white rabbits (n = 18, weight 2.2 ± 0.1 kg) were used in this study, and all of the experimental procedures were approved by the Experimentation Committee of the University of British Columbia. Two groups of animals were studied: (*1*) control group: rabbits infused with complement fragments (n = 9); (*2*) NO-treated group: rabbits infused with complement fragments with the inhalation of NO (n = 9).

Preparation of zymosan-activated plasma (ZAP). ZAP was used as a source of complement fragments and prepared by incubating heparinized rabbit plasma combined with zymosan A yeast (5 mg/ml plasma; Sigma Chemical, St. Louis, MO) at 37° C for 30 min (26). The plasma was centrifuged twice at 500 *g* for 10 min and the supernatant was stored at −20° C until use.

Measurement of PMN release from the bone marrow. To evaluate the effect of NO on PMN release from the bone marrow, the rapidly dividing myeloid cells in the bone marrow were labeled by injecting the thymidine analogue 5′-bromo-2′-deoxyuridine (BrdU) (100 mg/kg, Sigma Chemical) into the marginal ear vein at a concentration of 10 mg/ml in pyrogen-free saline over 15 min, 24 h before ZAP infusion. This allows PMN release from the bone marrow to be measured by observing the appearance of BrdU-labeled PMN in the peripheral blood (12, 27).

Experimental protocol. All rabbits were anesthetized with ketamine hydrochloride (35 to 50 mg/kg, intramuscularly) and xylazine (5 mg/kg, intramuscularly). Catheters were inserted into the superior vena cava via the jugular vein and into the aorta via the carotid artery. Rabbits were maintained sedated in a prone position with a continuous infusion of ketamine hydrochloride (20 to 25 mg/kg/h) and xylazine (4 to 6 mg/kg/h). Hemodynamic stability was maintained by an infusion of normal saline (∼ 20 ml/kg/h).

ZAP was infused into the marginal ear vein in both the control and the NO-treated groups at a rate of 1 ml/min for 15 min. NO inhalation (40 ppm) was started 10 min before the start of ZAP infusion in the NO-treated group (fraction of inspired oxygen [$F_{I_{O_2}}$] = 0.2, $NO_2 < 0.5$ ppm, measured with Pulmonox II; Pulmonox Medical Corporation, Alberta, Canada) and was continued throughout the experiment. The control group inhaled room air. Both groups were observed for 120 min and killed with an overdose of sodium pentobarbitone. The chest was opened rapidly, the base of heart was ligated to maintain the pulmonary blood volume, and lung samples were harvested for myeloperoxidase (MPO) measurement.

Blood sampling. Blood samples were collected simultaneously from the aorta and the superior vena cava to measure the arteriovenous (A-V) difference for white blood cells (WBC) and PMN counts across the lung, just before the start of NO inhalation (−10 min), just before ZAP infusion (0 min), and then at 2, 5, 10, 15, 20, 25, 30, 45, 60, 90, and 120 min after ZAP infusion. Blood volume was replaced with saline at each time point to maintain intravascular volume.

Processing of blood. Blood samples were collected in standard tubes containing potassium ethylene tetraacetic acid (EDTA; Vacutainer, Becton Dickinson, Rutherford, NJ). Blood cell counts were performed using a model SS80 Coulter Counter (Coulter Electronic, Hialeah, FL) and differential counts were made on Wright's stained blood smears. Blood used for the preparation of leukocyte-rich plasma (LRP) was collected in acid citrate dextrose. The RBC were sedimented by adding 4% dextran (average molecular weight 162,000; Sigma Chemical) in PMN buffer (1.38 mM NaCl, 27 mM KCl, 8.1 mM $Na_2HPO_4 \cdot 7\ H_2O$, 1.5 mM KH_2PO_4, and 5.5 mM glucose, pH 7.4). The resulting LRP was centrifuged to make cytospins on slides precoated with 3-aminopropyl-tri-ethoxysilane. These were then air dried and fixed in methanol before staining.

Detection of BrdU-labeled PMN (PMN^{BrdU}). A mouse monoclonal antibody to BrdU and the alkaline phosphatase antialkaline phosphatase (APAAP) method were used to detect the presence of BrdU in PMN in cytospins made of LRP (28). The cytospins were fixed in methanol and subjected to digestion in 0.04% pepsin for 15 min. The DNA was denatured by the incubation in 2 N HCl for 1 h. Nonspecific binding was blocked with 5% normal rabbit serum, and BrdU was bound with a mouse monoclonal anti-BrdU antibody (2 mg/ml; Dako Laboratories, Copenhagen, Denmark) for 1 h incubation. The first antibody was bound with the secondary antibody, rabbit anti-mouse IgG (Dako Laboratories) during 30 min incubation. Specific binding was detected by incubation with mouse monoclonal APAAP complex (Dako Laboratories) followed by a new fuchsin-based red substrate solution. The slides were counterstained with Mayer's hematoxylin, dehydrated, mounted, and coverslipped.

PMN with any nuclear stain were counted as positive (PMN^{BrdU}). PMN^{BrdU} were evaluated on a Nikon light microscope in random fields of view. The percentages of PMN^{BrdU} were determined by counting 100 PMN on a cytospin. Results are expressed as the percentage of PMN^{BrdU}.

MPO assay of lung tissue. MPO content of lung tissue was used to determine the relative number of PMN sequestered in the lung. Lung tissue samples from the control group (n = 9), the NO-treated group (n = 9), and untreated normal rabbits (n = 5) were evaluated. Lung tissues samples (300 mg) were homogenized in 1.5 ml of 0.5% of hexadecyltrimethylammonium bromide in 50 mM potassium phosphate buffer (pH 6.0) with detergent in an ice bath. Samples were sonicated to disrupt the granules and solubilize the MPO in the hexadecyltrimethylammonium bromide. Samples were then centrifuged at 3,000 *g* for 30 min at 4° C. Assay buffer comprised 750 μl of 1.7 mM H_2O_2 and 650 μl of 2.5 mM 4-aminoantipyrine with 2% phenol. An aliquot of 100 μl of supernatant of each sample was mixed into 1.4 ml of assay buffer at room temperature, and the change in absorbance at 510 nm over 1 min was recorded. Results are expressed as relative change in absorbance per minute at 510 nm. One unit of MPO was defined as causing a change of 1.0 absorbance and the data were expressed as U/g lung tissue.

In Vitro Studies

Cell preparation. Blood samples were collected from marginal ear artery of rabbits in acid citrate dextrose as an anticoagulant. LRP was prepared by sedimenting RBC using 4% dextran in PMN buffer as previously described. LRP was centrifuged and residual RBC were lysed by brief hypotonic shock with sterile water which was stopped with 2× phosphate-buffered saline (PBS; 2× PBS is 27 mM Na_2HPO_4, 132 mM KH_2PO_4, and 2.74 M NaCl). PMN were then separated from the mononuclear cells by centrifugation on Histopaque (Sigma Chemical), with a density of 1.077 g/ml at 150 *g* for 13 min. The PMN purity was > 95% with a viability of 98% as assessed by trypan blue exclusion.

F-actin content assay. Purified PMN were resuspended in Hanks' balanced salt solution (1.3 mM $CaCl_2$, 5.0 mM KCl, 0.3 mM KH_2PO_4, 0.5 mM $MgCl_2 \cdot 6\ H_2O$, 0.4 mM $MgSO_4 \cdot 7\ H_2O$, 138 mM NaCl, 4.0 mM $NaHCO_3$, 0.3 mM Na_2HPO_4; GIBCO-BRL, Gaithersburg, MD) at a concentration of 2.0 ± 0.1 × 10^6 /ml. In the control group, PMN were stimulated with 5% ZAP for 0, 15, 30, 60, 120, 180 and 240 s. In NO-treated groups, PMN were preincubated with NO donor, sodium nitroprusside (SNP) of different concentrations (10 μM, 100 μM, and

1 mM) for 10 min, and then stimulated with 5% ZAP using the same protocol as the control group. In all groups, the reaction was stopped by fixation using 3% paraformaldehyde for 30 min. After washing with PBS, PMN were simultaneously permeabilized and stained for 30 min in the dark at 37° C with a fresh mixture of 2 mM L-α-lysophosphatidylcholine, palmitoyl (Sigma) and 1 U/ml of BODIPY-phallacidine (Molecular Probes, Inc.). Cells were washed twice with PBS, and F-actin content was measured using a flow cytometer (Epics XL; Coulter Electronics, Hialeah, FL) and expressed as the mean fluorescent intensity of 3,000 cells. The increase of F-actin content was expressed as the percentage increase from the baseline value.

Deformability assay. PMN deformability was assessed by measuring the pressure needed to pass PMN through the polycarbonate filter with a uniform pore diameter of 5 μM (AMD Manufacturing Inc., Canada). We have used a modification of the *in vitro* filtration system described by Lennie and Lowe (29, 30). Purified PMN were suspended in 0.5% albumin containing Hanks' balanced salt solution at a concentration of $5.4 \pm 0.2 \times 10^5$/ml and filtered at a constant flow rate of 3 ml/min for 240 s using an infusion pump. The filtration pressure was measured upstream from the filter continuously by a pressure transducer (Validyne Engineering, Northridge, CA) and recorded every second by a computerized recording system. Three groups were studied: (*1*) PMN alone (PMN filtered in buffer); (*2*) PMN + ZAP group (PMN were stimulated with 5% ZAP for 2 min before filtration); (*3*) PMN + SNP + ZAP group (PMN were preincubated with 1 mM of SNP for 10 min and stimulated with 5% ZAP for 2 min before filtration).

Adhesion molecules study. Two activation-sensitive surface adhesion molecules, L-selectin and CD18, were measured. LRP was stimulated with 5% ZAP for 3 min and the expression of L-selectin and CD18 on PMN was measured using flow cytometry. In the control group, cells were stimulated with 5% ZAP for 3 min, and these were compared with the NO-treated groups; cells were preincubated with SNP at concentrations of 100 μM and 1 mM and S-nitrisoglutathione (GSNO) 100 μM or 1 mM for 10 min prior to the stimulation with 5% ZAP for 3 min. The reaction was stopped by diluting samples with large volume of PBS. Cells were incubated for 10 min with either 1 μg/ml of the mouse monoclonal antibody 60.3 (kindly donated by Dr. J. Harlan), DREG-200 (kindly donated by Dr. E. C. Butcher), or nonimmune mouse IgG. Cells were labeled for 10 min with 7.5 μg/ml of fluorescein isothiocyanate (FITC) conjugated goat anti-mouse secondary antibody (Sigma). The erythrocytes were lysed for 60 s with an immunolysing agent and leukocytes were fixed with PFA (commercial kit from Coulter Clone, Coulter Electronics). PMN were identified using the typical forward and side-scatter pattern and the expressions of L-selectin and CD18 were measured as mean fluorescent intensity of 3,000 cells. The changes of L-selectin and CD18 were expressed as the percentage changes from the baselines.

Statistics. Leukocyte, PMN counts, and A-V differences in circulating blood were analyzed using a two-way analysis of variance (ANOVA) with time as a repeating factor and NO-treated versus control as a grouping factor. The MPO content of lung tissue was analyzed using a one-way ANOVA. F-actin content and adhesion molecules of PMN were analyzed using a randomized block design ANOVA, with donor animal as a blocking factor. The pressure data of the filtration study were analyzed using paired two-tailed *t* tests of areas under the pressure curves. The sequential rejective Bonferroni test procedure was used to correct for multiple comparisons (31). A corrected p value < 0.05 was considered significant. All values are expressed as the mean ± standard error.

RESULTS

In Vivo Study

WBC and PMN counts. The circulating WBC and PMN counts (Figures 1A and 1B, respectively) show a biphasic leukocyte response after ZAP infusion. The WBC and PMN immediately decreased by a similar amount in both the control group (WBC: 6.2 ± 0.5 to 1.9 ± 0.2; PMN: 2.8 ± 0.4 to $0.1 \pm 0.02 \times 10^9$/ml) and the NO-treated group (WBC: 6.5 ± 0.5 to 2.4 ± 0.3; PMN: 3.1 ± 0.2 to $0.4 \pm 0.07 \times 10^9$/ml). This was followed by a rebound toward baseline levels after the ZAP infusion was stopped in both groups. The WBC and PMN of the control group decreased again by 2 h (WBC: 2.3 ± 0.3; PMN: $0.6 \pm 0.2 \times 10^9$/ml), although those of the NO-treated group remained near the baseline levels (WBC: 4.6 ± 0.9; PMN: $2.3 \pm 0.7 \times 10^9$/ml) ($p < 0.05$).

A-V difference of WBC and PMN counts. A-V differences of WBC and PMN counts across the lung show that the changes in the circulating cells were accompanied by a sequestration of PMN in pulmonary circulation after ZAP infusion (Figures 2A and 2B, respectively). Both in the control and the NO-treated group, A-V differences were seen during ZAP infusion. However, in the NO-treated group, A-V difference disappeared when ZAP was discontinued, whereas in the control group, A-V difference still remained ($p < 0.01$).

Figure 3 shows the calculated retention rates of unlabeled PMN and PMN^{BrdU} in the lung in the control (A) and the NO-treated (B) groups [(arterial count−venous count)/venous count × 100]. There was no difference in the retention rates between unlabeled PMN and PMN^{BrdU} in both groups.

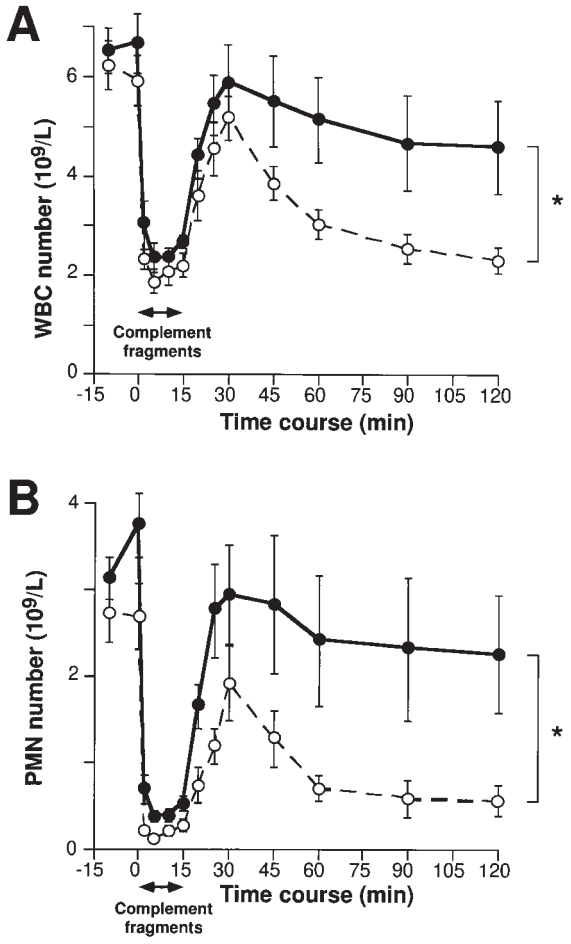

Figure 1. Effect of ZAP infusion and inhaled NO on leukocyte counts over the study period; circulating WBC (*A*), PMN counts (*B*). *Open circles* represent control group, *closed circles* represent NO-treated group. ZAP infusion immediately decreased WBC and PMN counts, which recovered to baseline values after ZAP infusion was stopped. Inhaled NO maintained WBC and PMN, whereas WBC and PMN decreased again in the control rabbits. Results are expressed as mean ± SEM of 9 animals for each groups. *$p < 0.05$ versus control for overall study period.

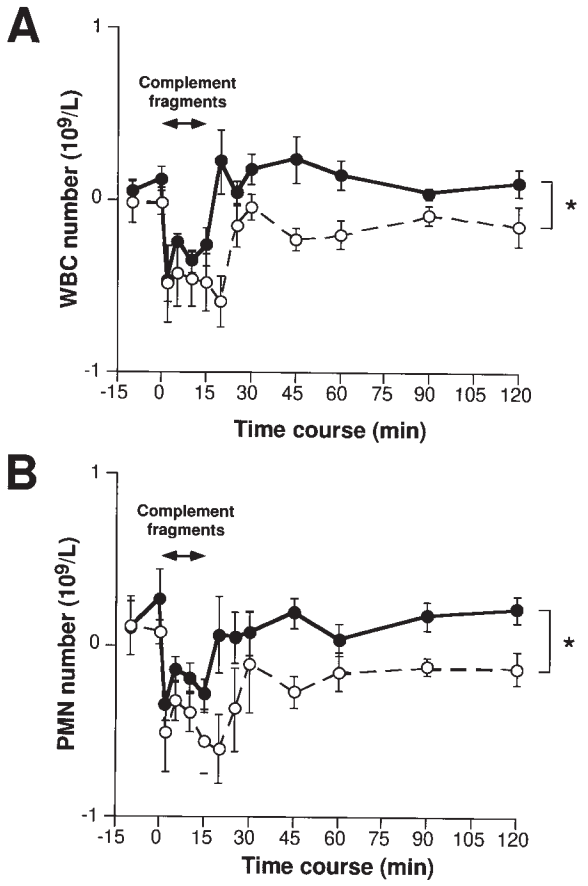

Figure 2. Effect of ZAP infusion and inhaled NO on A-V difference in WBC and PMN counts across the lung. A-V difference of WBC (*A*) and PMN counts (*B*). *Open circles* represent control group, *closed circles* represent NO-treated group. ZAP infusion produced A-V difference of WBC and PMN. A-V difference disappeared in NO-treated group after ZAP infusion was stopped, whereas the difference remained in controls. Results are expressed as mean ± SEM of 9 animals for each groups. *$p < 0.01$ versus control for overall study period.

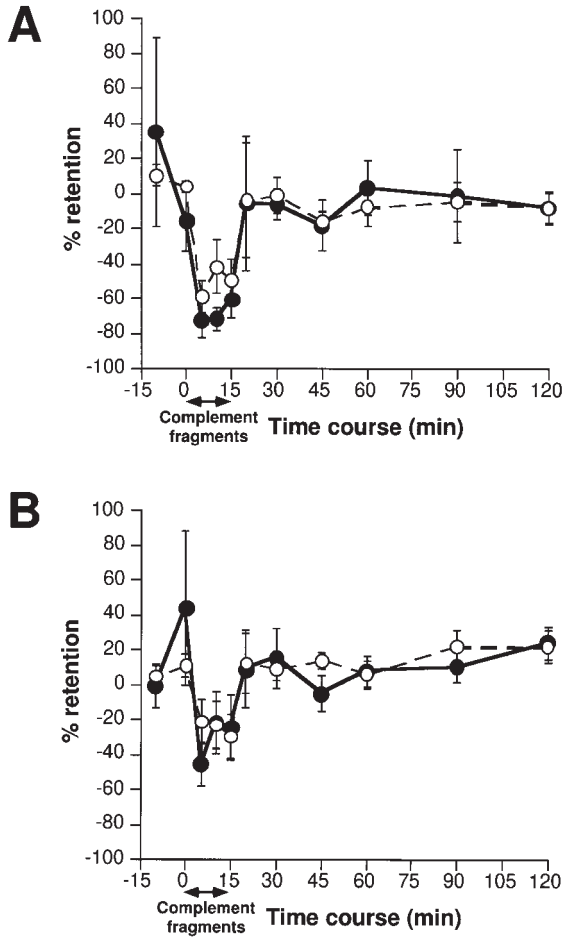

Figure 3. Effect of ZAP infusion and inhaled NO on retention of unlabeled PMN and PMN^{BrdU} in the lung in the control (*A*) and NO-treated (*B*) groups. *Open circles* represent unlabeled PMN, *closed circles* represent PMN^{BrdU}. ZAP infusion produced the retentions of both unlabeled PMN and PMN^{BrdU}. There were no differences between unlabeled PMN and PMN^{BrdU} in both groups. Results are expressed as mean ± SEM of 9 animals for each group.

Lung MPO content. Lung MPO content is consistent with excess PMN sequestration in lung tissue (Figure 4). MPO content increased after ZAP infusion compared with the values of normal rabbits (from 0.8 ± 0.2 to 1.5 ± 0.1 U/g lung, $p < 0.01$). Inhaled NO partially inhibited this increase (1.1 ± 0.1 U/g lung tissue, $p < 0.05$).

Bone marrow release of PMN. The circulating band cell population (Figure 5A) increased immediately after ZAP infusion and peaked at approximately 30 min, but there was no difference between the control and the NO-treated groups (control group: 1.5 ± 0.5 to 12.6 ± 3.1%; NO-treated group: 2.0 ± 0.6 to 13.6 ± 2.1%). Similarly, PMN^{BrdU} population (Figure 5B) increased immediately after ZAP infusion and peaked at approximately 30 min without a difference between the control and NO-treated groups (control group: 3.7 ± 1.0 to 33.7 ± 3.9; NO-treated group: 3.4 ± 0.6 to 30.2 ± 3.2%).

In Vitro Studies

F-actin content assay. F-actin content of PMN immediately increased, peaking at 30 s after ZAP stimulation (74 ± 4% increase from baseline) and remained high for the whole study period (Figure 6). Preincubation of PMN with SNP reduced this increase of F-actin content in a dose-dependent fashion (with 1 mM SNP, from 74 ± 4 to 57 ± 5% at 30 s, from 46 ± 1 to 27 ± 4% at 4 min, $p < 0.01$).

Deformability assay. The pressure required to pass PMN through 5-μm-pore polycarbonate membrane filters doubled after ZAP stimulation (8.3 ± 1.3 to 16.5 ± 2.3 cm H_2O at 4 min, $p < 0.01$, Figure 7). This was characterized by a steeper slope and higher plateau of the pressure curve. Preincubation of PMN with SNP (1 mM) reduced this increase in filtration pressure induced by ZAP stimulation (13.7 ± 2.0 cm H_2O at 4 min, $p < 0.05$). There was a small but nonsignificant dose-dependent effect of SNP (data not shown).

Adhesion molecules assay. The L-selectin expression of PMN was decreased by 50 ± 3% after ZAP stimulation ($p < 0.01$, Figure 8A). Preincubation of PMN with SNP (100 μM and 1 mM) had no effect on this response, indicating that NO did not alter the shedding off of L-selectin of PMN following ZAP stimulation.

The CD18 expression of PMN increased by 19 ± 2% after ZAP stimulation ($p < 0.01$, Figure 8B). Preincubation of PMN with SNP (100 μM and 1 mM) and GSNO (100 μM and 1 mM) inhibited this increase of CD18 expression ($p < 0.05$), indicat-

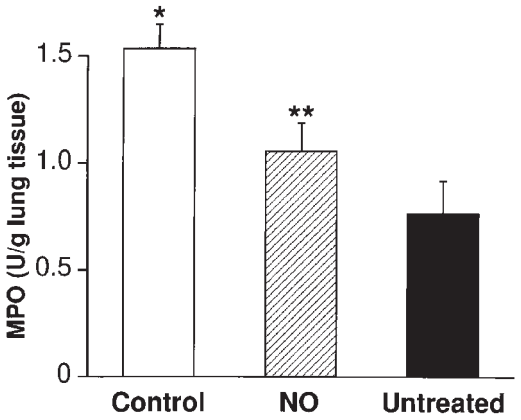

Figure 4. Effect of inhaled NO on PMN sequestration in the lung evaluated with MPO content of lung tissue. *Open column* represents control group, *hatched column* represents NO-treated group, and *closed column* represents untreated normal rabbits. MPO content increased after ZAP infusion. Inhaled NO reduced this increase of MPO content. Results are expressed as mean ± SEM of 9 animals for the control and NO-treated groups, 5 animals for normal untreated rabbits group. *$p < 0.01$ versus normal untreated, **$p < 0.05$ versus control group.

ing that NO prevented upregulation of CD18 expression of PMN after ZAP stimulation.

DISCUSSION

The results of this study show that inhaled NO reduces PMN sequestration that occurred in the lung after ZAP infusion. This was evident from the observation of the changes in circulating PMN over time, the decreased A-V difference of PMN across the lung, and the reduced MPO content in lung tissue of the NO-treated group. Because inhaled NO did not change PMN release from the bone marrow after infusion of complement fragments, we speculated that NO changes the deformability and adhesive qualities of PMN, both factors that influence PMN sequestration in the lung.

NO was given by inhalation *in vivo*, because inhaled NO does not change hemodynamic parameters such as systemic blood pressure and cardiac output which may affect PMN sequestration in the lung (32). The effects of NO on F-actin assembly, deformability change, and adhesion molecule expression of activated PMN were then examined *in vitro* to explore the mechanisms of the reduced PMN sequestration observed when NO was inhaled *in vivo*. *In vitro* NO was given using NO donors (SNP and GSNO) to assure continuous supply of NO to the PMN in solution and to avoid the activation of PMN by bubbling a gas through a solution containing PMN (33).

Infusion of complement fragments induced rapid PMN release from the bone marrow that peaked at 30 min. The release of PMN from the bone marrow could affect PMN sequestration in the lung because the number of PMN in the postmitotic pool of human bone marrow is 20 times that of the circulating blood (34). However, our results show that the release of PMN from this large pool was not changed by inhaled NO. Studies from our laboratory have shown that PMN newly released from the bone marrow preferentially sequester in the lung in the models of pneumonia, endotoxemia, and bacteremic infection (10–13). Interestingly, PMN released from the bone marrow by complement fragments sequestered similarly as circulating mature PMN (Figure 3), suggesting that these fragments released PMN from the bone marrow with similar

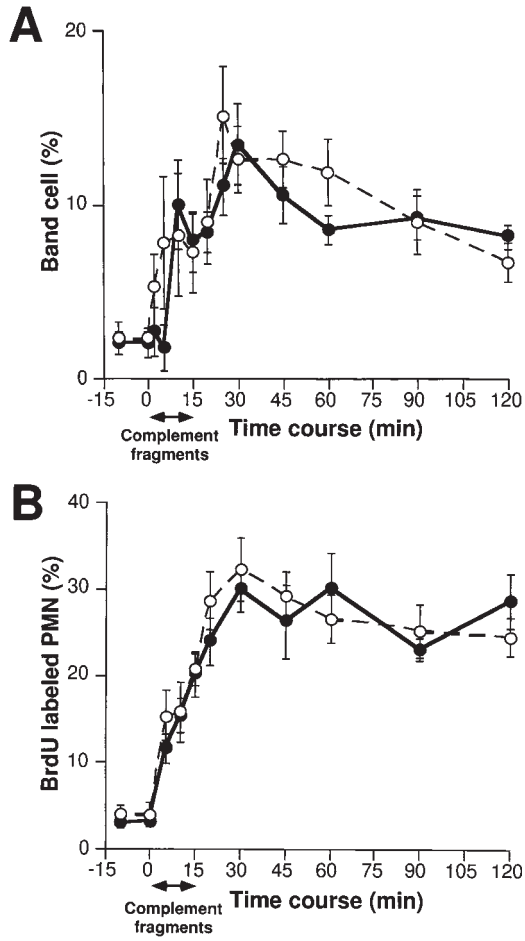

Figure 5. Effect of ZAP infusion and inhaled NO on PMN release from the bone marrow. Band cell percentage in circulation (*A*), BrdU-labeled PMN percentage (*B*). *Open circles* represent control group, *closed circles* represent NO-treated group. ZAP induced immediate release of PMN from the bone marrow. Inhaled NO did not change this release. Results are expressed as mean ± SEM of 9 animals for each group.

phenotypic and functional characteristics to circulating mature PMN. The failure of circulating PMN counts to increase during ZAP infusion in spite of the observed increase in PMN release from the bone marrow results from the sequestration of a large number of PMN in microvessels. The negative A-V difference of PMN counts across the lung during infusion of complement fragments also supports the concept that sequestration occurs in the lung (Figure 2). The circulating PMN counts increased transiently after the ZAP infusion was stopped, which is probably related to PMN release from the bone marrow, because the persisted A-V difference indicates that sequestered PMN were not demarginated from the lung (Figure 2). As inhaled NO did not change the complement fragments–induced PMN release from the bone marrow, we postulate that the reduced PMN sequestration induced by NO inhalation results from the effect of NO on PMN in the pulmonary microcirculation.

The sequestration of PMN in the lung is dependent on their size and deformability as well as the adhesive qualities of both PMN and endothelium (1, 4, 7). The rapid decrease in the deformability of activated PMN is the major factor responsible for PMN sequestration in the lung after infusion of comple-

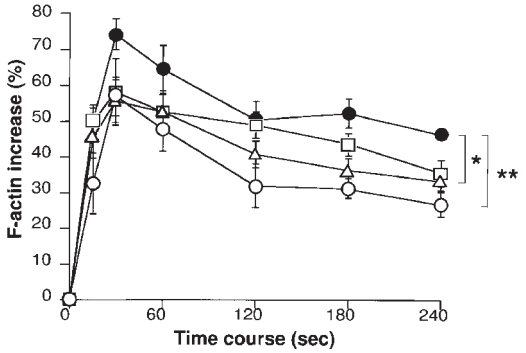

Figure 6. Effect of ZAP and NO on F-actin assembly of PMN measured by flow cytometry. PMN were stimulated with 5% ZAP with or without the preincubation of SNP. *Closed circles* represent PMN stimulated with ZAP (control). Other groups were pretreated with different concentrations of SNP (*open squares*: 10 μM; *open triangles*: 100 μM; *open circles*: 1 mM) and then stimulated with ZAP. ZAP induced immediate assembly of F-actin and NO partially inhibited this assembly in a dose-dependent fashion. Results are expressed as mean ± SEM of 6 experiments. *$p < 0.05$, **$p < 0.01$ versus control for overall study period.

ment fragments (6). Adhesion molecules play some role in prolonged sequestration of PMN in this model (9, 35). To explore the mechanisms of the reduction of PMN sequestration in the lung by NO, the effect of NO on PMN characteristics was evaluated *in vitro*. Complement fragments rapidly increases F-actin content in PMN to peak at 30 s, which remains higher compared with the baseline for 240 s. NO partially inhibits this increase in a dose-dependent fashion. Clancy and colleagues have shown an inhibitory effect of NO on F-actin assembly in PMN stimulated by 10^{-7} M formyl-methionyl-leucyl-phenylalanine (FMLP) (32). In their study, the inhibitory effect was rapid but transient, whereas in our study the inhibitory effect was maintained. They delivered NO by bubbling NO through the buffer. Because NO has a very short half-life in oxygenated solution, bubbled NO may be consumed and disappear quickly. Using NO donors like SNP, NO can be supplied continuously. Differences in the method of delivering NO and the differences in the type and dose of the activating stimulus may account for the discrepancy between our results and those from Clancy and colleagues (32). Changes in the cytoskeleton with F-actin assembly at the cell periphery, are thought to be responsible for the deformability change of PMN (6–8). Our filtration studies show that complement fragments decreases the deformability of PMN and NO partially inhibits this deformability change. This is consistent with the inhibition of F-actin assembly by NO. Therefore we conclude that NO inhibits the deformability change of activated PMN by inhibiting F-actin assembly in PMN.

Complement fragments stimulation sheds L-selectin and upregulates CD18 expression on PMN. NO inhibits CD18 upregulation without changing L-selectin response. This suggests that NO does not prevent selectin-mediated rolling of PMN but inhibits integrin-mediated firm adhesion of PMN to endothelial cells. This is in concordance with the report of Kubes and colleagues using an ischemia–reperfusion model of cats which showed that NO did not prevent selectin-dependent rolling but inhibited integrin-induced leukocyte adhesion in mesenteric venules (18). Adhesion molecules do not influence

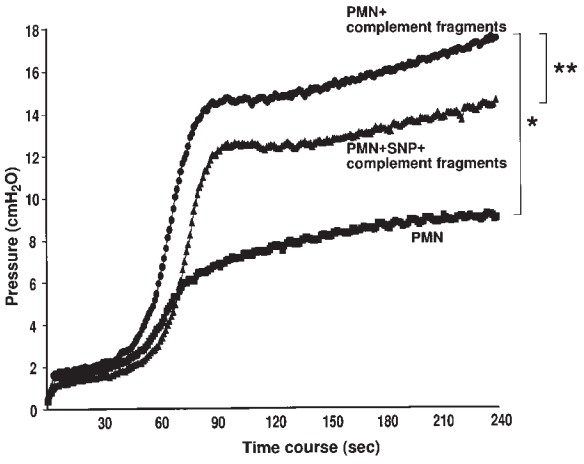

Figure 7. Effect of ZAP and NO on the deformability of PMN. PMN were stimulated with 5% ZAP with or without the preincubation of SNP (1 mM), and filtration pressure through 5-μm-pore polycarbonate membrane filter was measured. ZAP reduced the deformability of PMN. NO partially inhibited this change. Results are expressed as mean ± SEM of 8 experiments. *$p < 0.01$ versus PMN, **$p < 0.05$ versus PMN + ZAP.

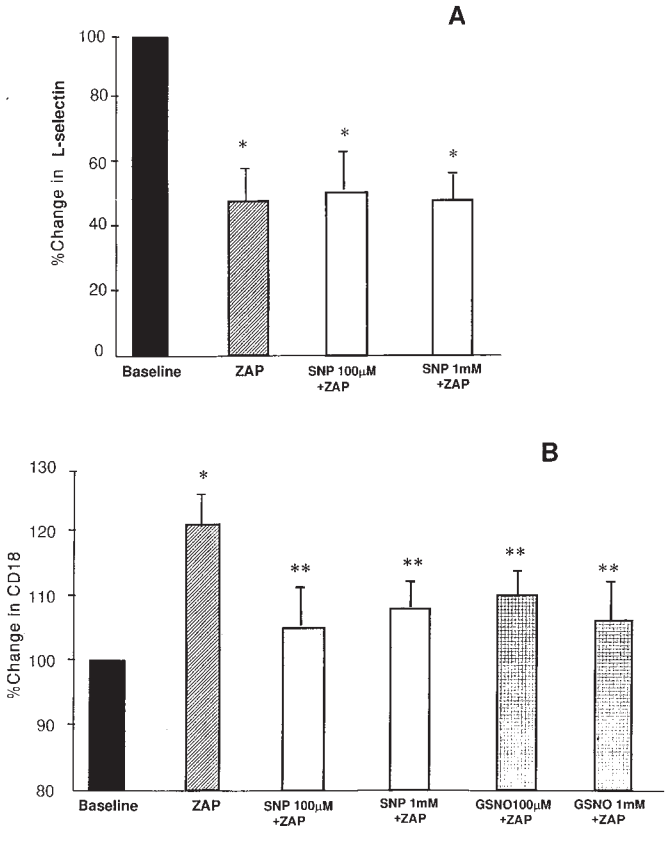

Figure 8. Effect of ZAP and NO on L-selectin (*A*) and CD18 (*B*) expression of PMN measured by flow cytometer. PMN were stimulated with 5% ZAP with or without the preincubation of SNP (100 μM or 1 mM) and GSNO (100 μM or 1 mM). ZAP decreased L-selectin expression of PMN. NO did not change this decrease. ZAP increased CD18 expression of PMN. Both the NO donors inhibited this increase. Results are expressed as mean ± SEM of 6 experiments. *$p < 0.001$ versus baseline, **$p < 0.05$ versus control (just ZAP).

the rapid PMN sequestration in the lung after ZAP infusion, but have an effect on the prolonged PMN retention in the lung (9, 35). Doerschuk and colleagues showed that the rapid sequestration of PMN in the lung with infusion of complement fragments is CD18-independent but that prolonged accumulation of PMN in lung microvessels is CD18-dependent (9). Similar results were obtained studying PMN sequestration in L-selectin-deficient mice (35). The effect of inhaled NO on the prolonged A-V difference of PMN across the lung (Figure 2) suggests that NO treatment changes PMN adhesiveness. This CD18 adhesiveness depends on both the number of CD18 surface molecules and the affinity for their ligand (37), and we postulate that NO reduces the adhesiveness of activated PMN by the inhibition of CD18-mediated adhesion.

There are several suggested mechanisms responsible for the inhibitory effect of NO on cellular functions. NO activates guanylate cyclase and increases the concentration of cGMP in the cell (38). cGMP is an inhibitory secondary messenger in PMN (39), which prevents the increase of intracellular Ca^{2+} by inhibiting Ca^{2+} influx through Ca^{2+} channel (40). The increase of intracellular Ca^{2+} plays important roles in signal transduction during PMN activation by activating cellular kinases and phosphatases which are important in F-actin assembly and integrin upregulation (41). Therefore, the prevention of Ca^{2+} influx by NO could prevent these responses during PMN activation. In addition, NO promotes adenosine diphosphate (ADP) ribosylation of actin which inhibits F-actin assembly (36). Furthermore, integrins are linked to F-actin via cytoskeletal proteins such as α-actinin, talin, vinculin, paxillin, and tensin and this foundation constructs signaling complexes. Signals through these complexes activate numerous components such as protein kinase C and mitogen-activated protein kinase, and increase intracellular Ca^{2+} (38) which causes feedback of integrin activation (39). Therefore, the inhibition of F-actin assembly by NO may affect this signal transduction, inhibit CD18 translocation to the cell surface and PMN activation. The reduced F-actin assembly and the inhibition of CD18 upregulation by NO observed in this study can be explained by these mechanisms. Besides, NO also changes the F-actin redistribution in endothelial cells (40), dilates capillary diameter (41), and reduces the expression of adhesion molecules on activated endothelium (42). We suspect that the inhibitory effects of NO on both PMN and endothelial functions are responsible for the observed reduction of PMN sequestration in the lung.

In summary, inhaled NO reduces PMN sequestration in the lung following infusion of complement fragments in rabbits. This reduction was not caused by the alteration of the rapid PMN release from the bone marrow following complement fragment infusion. *In vitro* studies suggest that NO reduces PMN sequestration in the lung by inhibiting deformability change of activated PMN via inhibition of F-actin assembly, and by reducing the adhesiveness of activated PMN via inhibition of CD18-mediated adhesion. We speculate that NO is an important regulator of PMN–endothelial interaction in inflammatory states, and that exogenous NO has potential therapeutic benefits in preventing PMN sequestration and PMN-mediated endothelial injury.

References

1. Hogg, J. C., and C. M. Doerschuk. 1995. Leukocyte traffic in the lung. *Ann. Rev. Physiol.* 57:97–114.
2. Downey, G. P., L. Fialkow, and T. Fukushima. 1995. Initial interaction of leukocytes within the microvasculature: deformability, adhesion, and transmigration. *New Horizons* 3:219–228.
3. Hogg, J. C. 1994. Felix Fleischner Lecture: the traffic of polymorphonuclear leukocytes through pulmonary microvessels in health and disease. *Am. J. Roentgenol.* 163:769–775.
4. Carlos, T. M., and J. M. Harlan. 1994. Leukocyte–endothelial adhesion molecules. *Blood* 84:2068–2101.
5. Hogg, J. C., H. O. Coxson, M. L. Brumwell, N. Beyers, C. M. Doerschuk, W. MacNee, and B. R. Wiggs. 1994. Erythrocyte and polymorphonuclear cell transit time and concentration in human pulmonary capillaries. *J. Appl. Physiol.* 77:1795–1800.
6. Inano, H., D. English, and C. M. Doerschuk. 1992. Effect of zymosan-activated plasma on the deformability of rabbit polymorphonuclear leukocytes. *J. Appl. Physiol.* 73:1370–1376.
7. Worthen, G. S., B. D. Schwab, E. L. Elson, and G. P. Downey. 1989. Mechanics of stimulated neutrophils: cell stiffening induces retention in capillaries. *Science* 245:183–186.
8. Frank, R. S. 1990. Time-dependent alterations in the deformability of human neutrophils in response to chemotactic activation. *Blood* 76: 2606–2612.
9. Doerschuk, C. M. 1992. The role of CD18-mediated adhesion in neutrophil sequestration induced by infusion of activated plasma in rabbits. *Am. J. Respir. Cell Mol. Biol.* 7:140–148.
10. Sato, Y., S. F. Van Eeden, D. English, and J. C. Hogg. 1998. Bacteremic pneumococcal pneumonia: bone marrow release and pulmonary sequestration of polymorphonuclear leukocytes. *Crit. Care Med.* 26:501–509.
11. Sato, Y., S. F. Van Eeden, D. English, and J. C. Hogg. 1998. Pulmonary sequestration of polymorphonuclear leukocytes released from the bone marrow in bacteremic infection. *Am. J. Physiol.* 275:L255–L261.
12. Lawrence, E., S. Van Eden, D. English, and J. C. Hogg. 1996. Polymorphonuclear leukocyte (PMN) migration in streptococcal pneumonia: comparison of older PMN with those recently released from the marrow. *Am. J. Respir. Cell Mol. Biol.* 14:217–224.
13. van Eeden, S. F., Y. Kitagawa, M. E. Klut, E. Lawrence, and J. C. Hogg. 1997. Polymorphonuclear leukocytes released from the bone marrow preferentially sequester in lung microvessels. *Microcirculation* 4:369–380.
14. Anggard, E. 1994. Nitric oxide: mediator, murderer, and medicine [see comments]. *Lancet* 343:1199–1206.
15. Beckman, J. S., and W. H. Koppenol. 1996. Nitric oxide, superoxide, and peroxynitrite: the good, the bad, and ugly. *Am. J. Physiol.* 271:C1424–1437.
16. Hickey, M. J., K. A. Sharkey, E. G. Sihota, P. H. Reinhardt, J. D. Macmicking, C. Nathan, and P. Kubes. 1997. Inducible nitric oxide synthase–deficient mice have enhanced leukocyte–endothelium interactions in endotoxemia. *FASEB J.* 11:955–964.
17. Clancy, R. M., and S. B. Abramson. 1995. Nitric oxide: a novel mediator of inflammation. *Proc. Soc. Exp. Biol. Med.* 210:93–101.
18. Kubes, P., I. Kurose, and D. N. Granger. 1994. NO donors prevent integrin-induced leukocyte adhesion but not P-selectin-dependent rolling in postischemic venules. *Am. J. Physiol.* 267:H931–H937.
19. O'Donovan, D. A., C. J. Kelly, H. Abdih, D. Bouchier-Hayes, R. W. Watson, H. P. Redmond, P. E. Burke, and D. A. Bouchier-Hayes. 1995. Role of nitric oxide in lung injury associated with experimental acute pancreatitis. *Br. J. Surgery* 82:1122–1126.
20. Ma, X. L., A. S. Weyrich, D. J. Lefer, and A. M. Lefer. 1993. Diminished basal nitric oxide release after myocardial ischemia and reperfusion promotes neutrophil adherence to coronary endothelium. *Circ. Res.* 72:403–412.
21. Kubes, P., and D. N. Granger. 1992. Nitric oxide modulates microvascular permeability. *Am. J. Physiol.* 262:H611–615.
22. Guidot, D. M., B. M. Hybertson, R. P. Kitlowski, and J. E. Repine. 1996. Inhaled NO prevents IL-1-induced neutrophil accumulation and associated acute edema in isolated rat lungs. *Am. J. Physiol.* 271:L225–229.
23. Bloomfield, G. L., S. Holloway, P. C. Ridings, B. J. Fisher, C. R. Blocher, M. Sholley, T. Bunch, H. J. Sugerman, and A. A. Fowler. 1997. Pretreatment with inhaled nitric oxide inhibits neutrophil migration and oxidative activity resulting in attenuated sepsis-induced acute lung injury [see comments]. *Crit. Care Med.* 25:584–593.
24. Doerschuk, C. M., M. F. Allard, and J. C. Hogg. 1989. Neutrophil kinetics in rabbits during infusion of zymosan-activated plasma. *J. Appl. Physiol.* 67:88–95.
25. Terashima, T., B. Wiggs, D. English, J. C. Hogg, and S. F. van Eeden. 1996. Polymorphonuclear leukocyte transit times in bone marrow during streptococcal pneumonia. *Am. J. Physiol.* 271:L587–592.
26. Bicknell, S., S. van Eeden, S. Hayashi, J. Hards, D. English, and J. C. Hogg. 1994. A non-radioisotopic method for tracing neutrophils *in vivo* using 5′-bromo-2′-deoxyuridine. *Am. J. Respir. Cell Mol. Biol.* 10: 16–23.
27. Lennie, S. E., G. D. O. Lowe, J. C. Barbenel, C. D. Forbes, and W. S.

Foulds. 1987. Filterability of white blood cell subpopulations separated by an improved method. *Clin. Hemorheol.* 7:811–816.
28. Lowe, G. D. 1987. Blood rheology in vitro and in vivo. *Baillieres Clin. Haematol.* 1:597–636.
29. Holland, B. S., and M. D. Copenhaver. 1987. An improved sequential rejective Bonferroni test procedure. *Biometrics* 42:417–423.
30. Bainton, D. F. 1980. The cells of inflammation: a general review. *In* G. Weissman, editor. The Cell Biology of Inflammation. Elsevier/North Holland, New York. 1–25.
31. Doyle, N. A., S. D. Bhagwan, B. B. Meek, G. J. Kutkoski, D. A. Steeber, T. F. Tedder, and C. M. Doerschuk. 1997. Neutrophil margination, sequestration, and emigration in the lungs of L-selectin-deficient mice. *J. Clin. Invest.* 99:526–533.
32. Clancy, R., J. Leszczynska, A. Amin, D. Levartovsky, and S. B. Abramson. 1995. Nitric oxide stimulates ADP ribosylation of actin in association with the inhibition of actin polymerization in human neutrophils. *J. Leukocyte Biol.* 58:196–202.
33. Dzau, V. J., G. H. Gibbons, and P. C. Lee. 1994. Novel drug targets in vascular pathobiology. *In* B. N. Singh, P. M. Vanhoutte, V. J. Dzau, and R. L. Wooseley, editors. Cardiovascular Pharmacology and Therapeutics. Churchill Livingstone, New York. 317–324.
34. Schroder, H., P. Ney, I. Woditsch, and K. Schror. 1990. Cyclic GMP mediates SIN-1-induced inhibition of human polymorphonuclear leukocytes. *Eur. J. Pharmacol.* 182:211–218.
35. Milbourne, E. A., and F. L. Bygrave. 1995. Do nitric oxide and cGMP play a role in calcium cycling? *Cell Calcium* 18:207–213.
36. Mandeville, J. T., and F. R. Maxfield. 1996. Calcium and signal transduction in granulocytes. *Curr. Opin. Hematol.* 3:63–70.
37. Schleiffenbaum, B., E. Moser, M. Ptarroyo, and J. Fehr. 1989. The cell surface glycoprotein Mac-1 (CD11b/CD18) mediates neutrophil adhesion and modulates degranulation independently of its quantitative cell surface expression. *J. Immunol.* 142:3537–3545.
38. Clark, E. A., and J. S. Brugge. 1995. Integrins and signal transduction pathways: the road taken. *Science* 268:233–239.
39. Sjaastad, M. D., and W. J. Nelson. 1997. Integrin-mediated calcium signaling and regulation of cell adhesion by intracellular calcium. *Bioessays* 19:47–55.
40. Liu, S. M., and T. Sundqvist. 1995. Involvement of nitric oxide in permeability alteration and F-actin redistribution induced by phorbol myristate acetate in endothelial cells. *Exp. Cell Res.* 221:289–293.
41. Bloch, W., D. Hoever, D. Reitze, L. Kopalek, and K. Addicks. 1995. Exogenously supplied nitric oxide influences the dilation of the capillary microvasculature in vivo. *Agents Actions Suppl.* 45:151–156.
42. De Caterina, R., P. Libby, H. B. Peng, V. J. Thannickal, T. B. Rajavashisth, M. A. Gimbrone, Jr., W. S. Shin, and J. K. Liao. 1995. Nitric oxide decreases cytokine-induced endothelial activation: nitric oxide selectively reduces endothelial expression of adhesion molecules and proinflammatory cytokines. *J. Clin. Invest.* 96:60–68.